Basins of attraction in driven dynamical systems

E. Eschenazi, H. G. Solari, and R. Gilmore
Department of Physics and Atmospheric Science, Drexel University, Philadelphia, Pennsylvania 19104
(Received 18 April 1988)

The organization of multiple coexisting basins of attraction in two-dimensional driven dynamical systems is studied. This study is carried out, in particular, for the laser with modulated parameter and the Hénon map. Basin organization is governed primarily by the ordering of heteroclinic and homoclinic connections of regular saddles. This organization is complex yet systematic, with accumulation structures governed by the order of saddle connections. We study the evolution of a basin in the presence of multiple coexisting basins, from (before) birth to (beyond) death. Many of the processes that occur are canonical. These include the reorganization of existing basins in preparation for the creation of a new basin by saddle-node bifurcation, the increased intertwining, in Poincaré section, of the components of a basin, and the increased wrinkling of each component as the basin evolves from birth to death. These also include the processes that mark disintegration and the ultimate demise of the basin, beginning at homoclinic tangency and terminating in its disappearance or enlargement in a crisis.

I. INTRODUCTION

Extensive experimental investigations have been carried out on laser systems in various configurations in order to shed additional light on the behavior of nonlinear dynamical systems.[1-8] One configuration which has been extremely convenient for such studies has been the laser with modulated parameters. The usefulness of this system arises, on the experimental side, from its stable behavior under a wide range of operating conditions[1,2] and its extremely fast response time compared with fluid systems (milliseconds compared to hours, days, or weeks) and, on the theoretical side, from the existence of a very simple model which describes the behavior of the system. The model equations are[6]

$$\begin{aligned}\frac{dx}{dt}&=[z-R\cos(\Omega t)]x\ ,\\ \frac{dz}{dt}&=(1-\epsilon_1 z)-(1+\epsilon_2 z)x\ ,\end{aligned}\tag{1.1}$$

where x represents the laser output intensity, z the population inversion, and Ω the driving frequency of the electro-optic modulator. The experimental, theoretical, and numerical properties of this system have been described extensively elsewhere.[6,9,10]

A complete understanding of this system must involve a deep understanding of three types of structures. These are (a) the periodic orbits, both stable and unstable; (b) the basins of attraction which surround the stable attractors; and (c) the boundaries which separate basins.

We must understand each of these three structures at two levels, a kinematic and a dynamic level.

At the kinematic level, we must understand (a) how to characterize their components; (b) how they are organized; (c) their multiplicity; (d) their topological properties; and (e) their scaling properties. At the dynamical level, we must understand (a) how each comes into existence, (b) evolves, and (c) is finally destroyed.

We must also understand the precursors to the birth of each structure, as well as the residuals after its death. We must finally understand how the basins are organized around the stable orbits, and the boundaries around the basins.

Many of these questions have now been resolved for the periodic orbits of the laser system (1.1) and, by extension, for other two-dimensional driven damped dynamical systems.[11] The dynamics are organized by a Smale horseshoe. The formation of the horseshoe in a Poincaré section governs the development and organization of the spectrum of periodic orbits, both stable and unstable. A matrix of topological indices, the relative rotation rates, has been introduced to describe the global organization of these orbits. These indices, related to the flow, are determined up to a single overall integer by the horseshoe map. This integer is the relative rotation rate of the two period-1 orbits.

The relative rotation rates have been useful for identifying different orbits with the same periodicity which have been observed in the laser. For example, two distinct period-5 orbits have been observed. One is clearly a Newhouse orbit, the other is not. The logical sequence name of the second orbit provided a tentative identification of this orbit which was confirmed by computation of its relative rotation rates with all coexisting orbits.[10]

We turn our attention in the present work to an understanding of the basins of attraction of the laser system. Our understanding of the properties of basins has evolved by studying the basins of the laser flow (1.1) and those of the Henon orientation-preserving map[12]

$$\begin{aligned}x'&=a-Jy-x^2\ ,\\ y'&=x\ .\end{aligned}\tag{1.2}$$

The return map of the laser appears to belong to the same

class of mappings as the Hénon map, since the two dynamical systems have the same hyperbolic horseshoe. As a result, the general qualitative features of the laser map, which can be obtained only after extensive numerical integration, are more readily obtained from the Hénon map. The map (1.2) has been particularly useful for studying the precursors to saddle-mode bifurcation, where numerical studies are bedeviled by long-term transients.

Knowledge of basin organization is necessary to predict the statistics of basin occupation under a variety of initial conditions. For example, if the initial time evolution of an orbit shows transients of several different periods, we would like to be able to predict the probability distribution for the final state to occur in each of the accessible basins. As another example, if a system has coexisting orbits[9] of periods 1,3,4,5, . . . and the initial state is in the period-4 basin, we may ask for the statistics of the final state when the period-4 orbit is destroyed by changing a control parameter. Both questions can be addressed only after the organization of coexisting basins of attraction is known.

In the present work we study the local and global organization of basins of attraction. This organization is governed by a very small number of constraints. These constraints, discussed in Sec. II, involve heteroclinic and homoclinic saddle connections and the order in which these crossings occur. The global organization of basins is discussed in Sec. III. This organization is modified by the birth and death of individual basins. The evolution of a basin, from (before) birth to (after) death, is described in Secs. IV–VI. We study the precursors to its birth in a saddle-node bifurcation and the properties of a basin at its birth in Sec. IV. The evolution of a basin, including its increased wrinkling due to impending homoclinic tangencies, is studied in Sec. V. Its old age, disintegration in a homoclinic tangency, death in a crisis, and the remnants of the basin after its death, are described in Sec. VI. In Sec. VII we discuss several additional properties of basins of attraction.

Of course, different nonlinear dynamical systems differ in detail—that is why they are so interesting. However, many features are common throughout an entire class of systems. In this work we discuss those features which are common to the class of two-dimensional periodically driven damped dynamical systems whose dynamics are governed by the development of a hyperbolic horseshoe. This class includes a number of important models of laser systems which have been studied both experimentally and theoretically.

II. INVARIANT SETS AND THEIR CONSTRAINTS

For the laser (1.1) all attractors belong to a branch born in a saddle-node bifurcation except for the attractor belonging to the period-1 branch.[9–11] In the period-1 case, the period-1 saddle inset is the line $x=0$, which separates the basins of all bounded motion (the physical states with $x>0$) from the basin of "infinity" (the unphysical states with negative intensity, $x<0$). For the Hénon map (1.2) similar statements apply, except that even the period-1 attractor is born in a saddle-node bifurcation. We define periodic attractor as a periodic orbit with a neighborhood N of initial conditions that remain in N under forward iteration and converge toward the attractor in the limit of the time going to infinity.[13]

The properties of the basins of attraction are largely determined by the insets and outsets of the regular periodic saddles. We define the basin of attraction as the set of points that map into the neighborhood N of the periodic attractor under forward iteration, i.e., the union of the preimages of N. The insets are important since they form part of the basin boundary of the corresponding attractor until that attractor is annihilated in a crisis. The outsets are important since a single homoclinic or heteroclinic crossing of stable and unstable invariant sets requires a countable number of additional crossings. This in turn causes extensive bending and folding of both. The basins of the coexisting attractors of periods 1, 2, and 3 of the laser are shown in Fig. 1. The saddles and boundaries are clearly marked; these boundaries oscillate extensively because the insets intersect the outset of the period-1 regular saddle. The boundary *between* two sets U and V is the intersection of their closures: $\partial(U,V)=\overline{U}\cap\overline{V}$. Equivalently, it is the set of points p with the property that every ϵ neighborhood of p has nonzero intersection with both U and V: $N(p,\epsilon)\cap U\neq\emptyset$, $N(p,\epsilon)\cap V\neq\emptyset$. The boundary of a set U is the boundary between U and its complement: $\partial U=\overline{U}\cap\overline{U}^c$.

The inset of the period-p regular saddle consists of two components, ps_L and ps_R, separated by the saddle (Fig. 2). Each component is two sided, in the sense that every neighborhood of a point in it always has nonzero intersection with the basin on the same side of the inset. Facing the direction of flow toward the saddle, this preferred side remains always on the left of one component (ps_R)

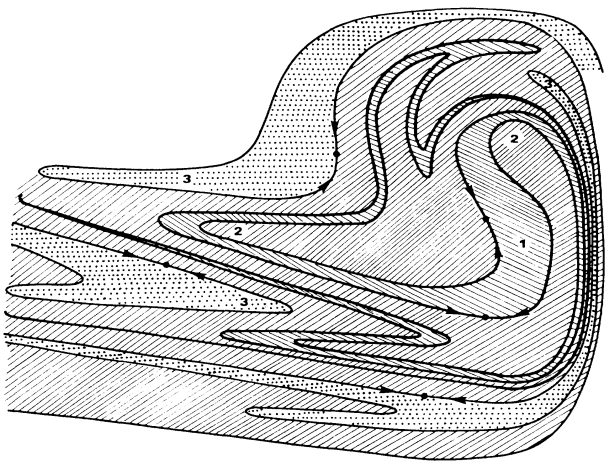

FIG. 1. Basins of coexisting attractors for the laser equations (1.1) with $R=0.7$, $\epsilon_1=0.03$, $\epsilon_2=0.009$, $\Omega=1.5$. The saddles of periods 1, 2, and 3 are shown. The boundary between the period-1 and -2 basins is the period-2 saddle inset; the boundary between the period-2 and -3 basins is the period-3 saddle inset. The boundaries of the basins of period 1, 2, and 3 are, respectively, $1s\cup 2s$, $1s\cup 2s\cup 3s$, and $1s\cup 3s$.

and on the right for the other (ps_L), as shown in Fig. 2. In a sense, the right-hand boundary of the period-p basin is ps_R, the left-hand boundary is ps_L.

The outset of the period-p saddle consists also of two components, pu_I and pu_E, separated by the saddle (Fig. 2). Immediately following the saddle-node bifurcation one component (pu_I) lies completely within the basin of attraction, while the other (pu_E) is completely outside. The interior component is intimately involved in the period-doubling cascade (Fig. 3). It undergoes a homoclinic tangency associated with the cascade, followed eventually by heteroclinic tangencies with insets of other regular saddles as the period-p horseshoe is formed. The exterior component is involved in the heteroclinic crossings described below; these are followed by a homoclinic crossing as the horseshoe is formed.

When the stable-invariant set of the regular period-p saddle (ps) crosses the (exterior) unstable-invariant set of the regular period p' saddle (ps_L or $ps_R \times p'u_E$), the invariant set ps accumulates on the stable-invariant set of the regular period p' saddle, and conversely:[13]

$$\begin{array}{ccc} & ps \times p'u & \\ \swarrow & & \searrow \\ \overline{ps} \supset p's & & pu \subset \overline{p'u} \end{array} . \tag{2.1}$$

These accumulation relations are shown in Fig. 4. We are able to make precise statements about the crossing relations for a particular class of periodic orbits generated by the development of a Smale horseshoe in the laser and Henon systems. These are the Newhouse orbits,[14] which are the principal periodic orbits seen in laser experiments.[1-9] We have observed the following crossing relations:[15,16]

$$\begin{array}{ll} 3s_L \times 4u_E & 3s_R \times 4u_E \\ 4s_L \times 5u_E & 4s_R \times 5u_E \\ 5s_L \times 6u_E & 5s_R \times 6u_E \\ 6s_L \times 7u_E & 6s_R \times 7u_E \\ \vdots & \vdots \\ 1u_I \times ps_L & 1u_I \times ps_R \ . \end{array} \tag{2.2}$$

These crossings occur whenever the saddles of periods p and $p+1$ exist. A heuristic reason for the existence of these crossings is shown in Fig. 5. The crossing $1u \times ps$ implies that all stable insets ps accumulate on $1s$, the boundary between bounded orbits in phase space and the attractor at "infinity." This in turn implies that the basin of the period-p branch accumulates on the boundary of the attractor at infinity, for each p. This in turn requires that the coexisting basins of attraction must be intertwined in a rather complicated way.

There is a reverse sequence of crossings:[16,17]

$$\begin{array}{l} 3u_I \times 4s_L \text{ or } 4s_R \\ 4u_I \times 5s_{\text{same}} \\ 5u_I \times 6s_{\text{same}} \\ 6u_I \times 7s_{\text{same}} \\ \vdots \end{array} \tag{2.3}$$

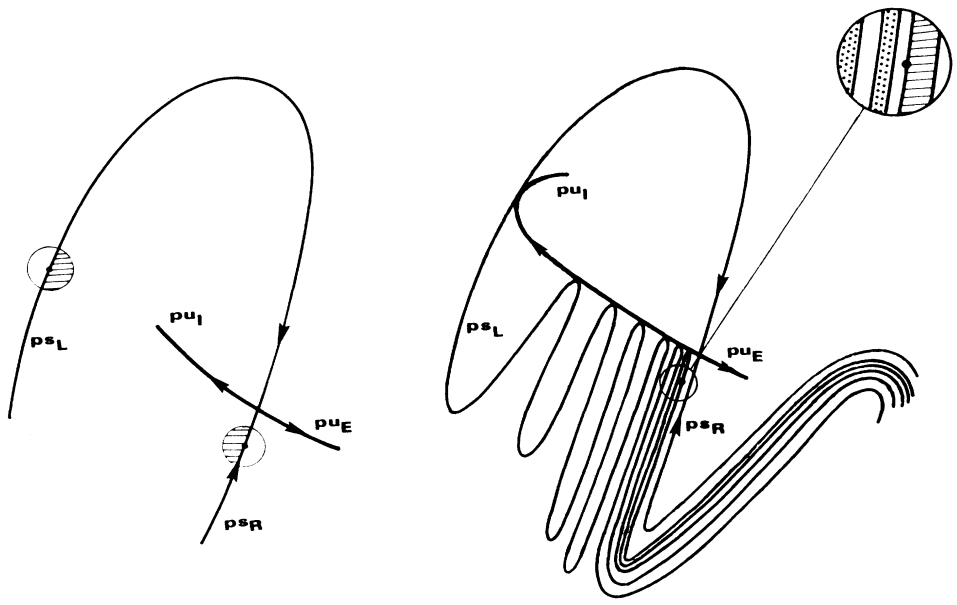

FIG. 2. A regular saddle has a stable invariant set with two components. Each component is two sided, in the sense that every neighborhood of any point of ps_L or ps_R always has a nonempty intersection with the basin on the same side, as long as the basin exists. If the basin is sufficiently convoluted (right), there may be nonzero intersections on the other side as well, as shown in the inset. The additional nonzero intersection is shown dotted.

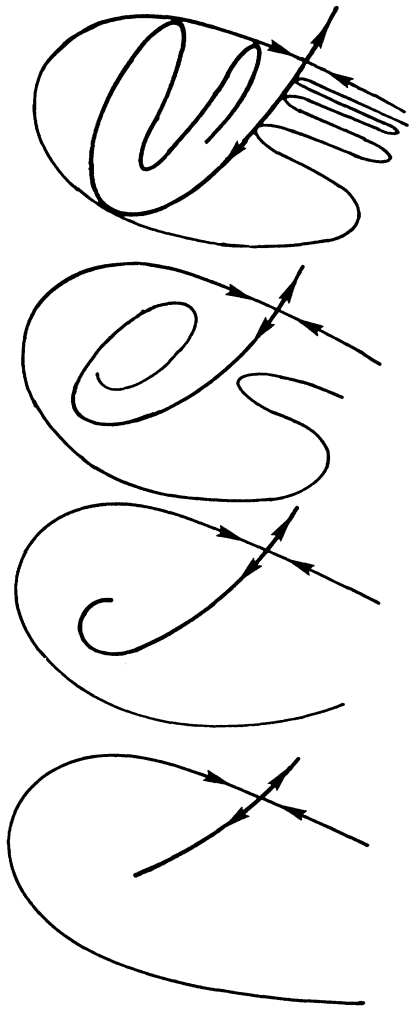

FIG. 3. The interior unstable component of the period-p saddle is involved in the period-doubling cascade based on the period-p branch.

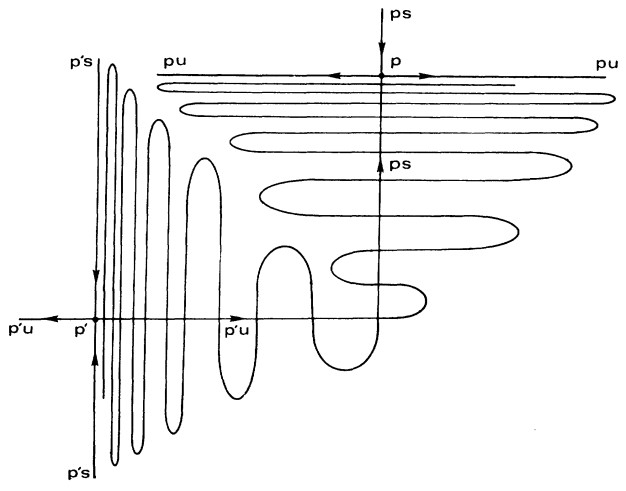

FIG. 4. A single saddle crossing requires an infinite number of additional crossings. Here $ps \times p'u$, requiring $pu \subset \overline{p'u}$ and $p's \subset \overline{ps}$.

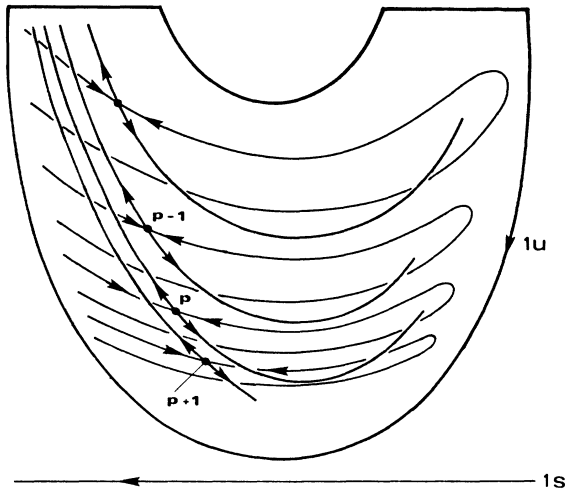

FIG. 5. Saddle-node bifurcations occur systematically in the fingers of the outset of the period-1 saddle. In this formation process, $(p+1)u_E$ crosses ps_R (for the orientation shown) whenever both saddles exist. For sufficiently high periods, the reverse crossing also takes place. In this figure $pu_I \times (p+1)s_L$ but $(p-1)u_I$ does not cross ps_L.

These crossings do not always occur, but for some p_0, they occur for all $p > p_0$, as indicated in Fig. 5. As the homoclinic tangency approaches, $p \to \infty$. At and beyond the homoclinic tangency $1s \times 1u_I$, there is the additional set of crossings

$$1s \times pu \quad (p > p_0) .$$

For Newhouse orbits the value of p_0 decreases as the homoclinic tangency of the period-1 saddle approaches and is passed.

When two or more basins of attraction coexist, the order of crossing of the invariant sets of their regular saddles provides a natural ordering for the saddles themselves.[18] This is important because the order of the saddles is responsible for the organization of the basins among themselves. We can define order either dynamically or topologically. We define saddle A to precede saddle B, or say A is interior to B, or write $A \leq B$, if almost every point in the inset of A approaches the inset of B arbitrarily closely under reverse iteration (or flow). Equivalently, A precedes B if the inset of A accumulates on the inset of B: $\overline{As} \supset Bs$. The reasons for the term "is interior to" will be made clearer in Sec. III. Saddle order is transitive: if $A \leq B$ and $B \leq C$ then $A \leq C$. Saddle ordering is illustrated in Fig. 6.

The crossings given in (2.2) determine the saddle order: $3 \leq 4 \leq 5 \leq \cdots \leq 1$. This order, together with the fact that the period-3 basin lies between $3s_L$ and $3s_R$, which both accumulate on $4s_L$ and $4s_R$, which in turn accumulate on $5s_L$ and $5s_R, \ldots$, determines the basin organization.[18] The period-3 basin accumulates on the period-4 basin, and so on, all accumulating on the inset of the period-1 saddle.

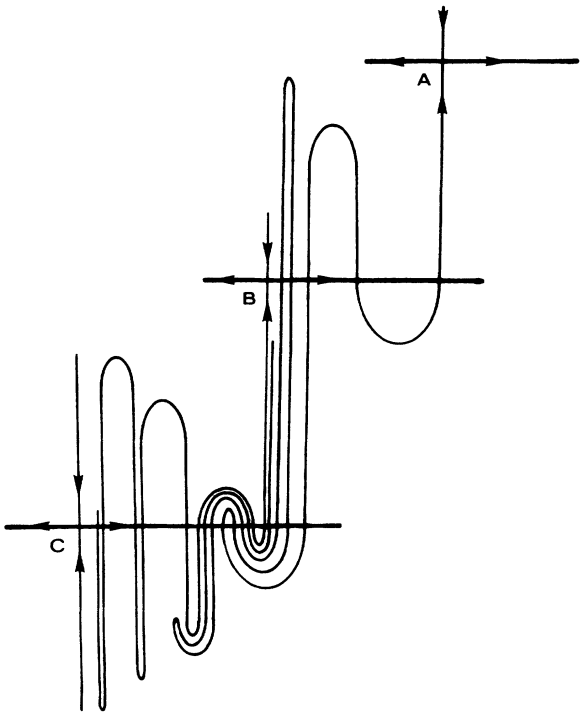

FIG. 6. The saddle inset of A accumulates on the saddle inset of B, and B on C, so that A precedes B precedes C or $A \leq B \leq C$. In fact, the accumulation is much more complicated, since the inset of B, as it accumulates on the inset of C, carries with it the inset of A.

When some of the reverse crossings indicated in (2.3) occur (e.g., $4u \times 5s$, $5u \times 6s$, $6u \times 7s$), they determine the saddle order: $4 \geq 5 \geq 6 \geq 7$. In this case the saddles become equivalent in the sense that the inset of each accumulates on all the others. Any of these basins of attraction which exist are intertwined in a very complicated manner.

III. GLOBAL ORGANIZATION OF BASINS

In this section we describe the global organization of multiple coexisting basins of attraction in the flow (1.1) and the map (1.2). This is done to set the stage for the description, in the following sections, of what occurs when new basins of attraction are created when multiple basins already exist.

In the flow (1.1), the basin of each period-p stable-invariant set is a connected open set which is not simply connected. In Poincaré section, and in the map (1.2), each period-p basin consists of p disjoint connected and simply connected open sets. This remains true as the period-p attractor evolves through its usual evolutionary process (period-doubling cascade, accumulation, noisy period-halving inverse cascade, etc.). A point belonging to a period-p regular saddle exists in each of the p components of the basin boundary. Both two-sided components of each regular period-p saddle inset form part of the boundary of each of the p components of the period-p basin.

The organization of the period-3 basin within that of the period-1 attractor of the Henon map is shown schematically in Fig. 7. Since $1u_I \times 3s_L$ and $3s_R$ [Eq. (2.2)], both components of the inset of the regular period-3 saddle accumulate on the stable-invariant manifold of the period-1 saddle. These two components alternate as they accumulate on $1s$ ($1s_L$ and $1s_R$), alternatively confining the period-3 basin between $3s_L$ and $3s_R$ and its complement, the period-1 basin, between $3s_R$ and $3s_L$. This alternation is shown in the inset of Fig. 7.

The period-3 basin is formed within the original period-1 basin. Iterating backwards, the three components of the period-3 basin spiral outwards toward the boundary of the attracting region and the attractor at infinity, with the transverse sections becoming increasingly thin as accumulation is approached.

The global organization of the period-4 basin is similar to that of the period-3 basin. However, when the period-1, -3, and -4 basins coexist, their organization is as shown schematically in Fig. 8. The invariant sets $3s_R$ and $3s_L$ accumulate on $4s$ (both) which, in turn, accumulate on $1s$, carrying $3s$ with it. The components $4s_L$ and $4s_R$ enclose the period-4 basin, while $4s_R$ and $4s_L$ enclose the complement. The complement consists of the intertwined period-1 and -3 basins, which accumulate on $4s$. The accumulation structure of the intertwined basins is illustrated in Figs. 8(b) and 8(c). In Fig. 8(b) we take a line segment between two successive strips of the period-4 basin

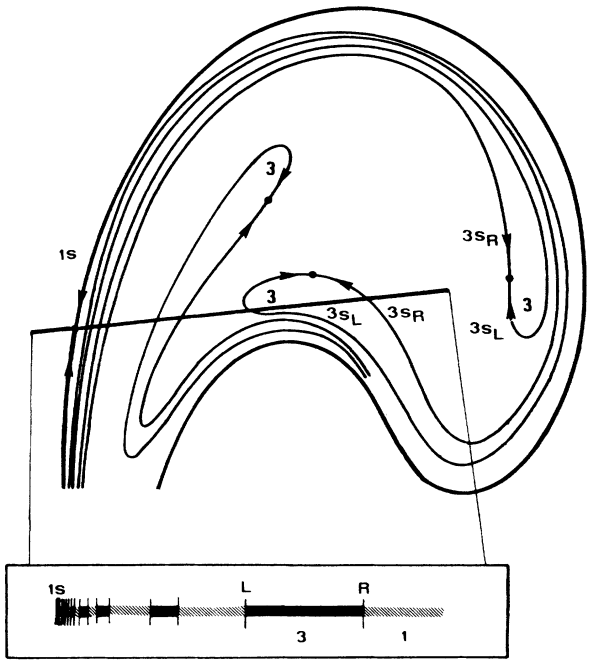

FIG. 7. The period-3 basins spiral outward (in reverse iteration) in the fashion shown, to accumulate on $1s$. The period-3 basin is contained between the saddle insets $3s_L$ and $3s_R$ while its complement in the bounded region, the period-1 basin, is contained between $3s_R$ of one component and $3s_L$ of the preimage component. The inset shows the alteration of basins as they accumulate on $1s$.

and look at the organization of the period-1 and -3 basins as they intersect the segment. In Fig. 8(c) we take a segment between the invariant sets $4s$ and $1s$ and look at the organization of the basin structure along that segment.

Iterating backwards, the four components of the period-4 basins spiral outwards toward the boundary of the attracting region. The three components of the period-3 basins also spiral outward. Whenever one of them "gets between" a component of the period-4 basin and the boundary, $1s$, of the attracting region, it is folded back around the period-4 component so that this component gets between the period-3 basin and $1s$ (cf. Ref. 16). This extensive folding is required by the crossing $4u_E \times 3s_L$ and $3s_R$ and results in the accumulation of $3s$ on $4s$ while in addition $4s$ accumulates on $1s$. In a very real sense, the period-3 saddle "is interior to" the period-4 saddle, . . . , which in turn "is interior to" the period-1 saddle.

Although the intertwining among basins is complicated, it is highly organized. The organization is completely determined by the accumulation organization of the stable-invariant insets [Eq. (2.2)], which in turn is determined by the saddle order. For example, $3s$ accumulates on $4s$ which accumulates on $1s$, or $3s \supset 4s \supset 1s$, which is required by the saddle order $3 \leq 4 \leq 1$. To illustrate this simplicity in complexity, we show in Fig. 9 the organization of the basins of attraction of coexisting Newhouse orbits of periods 6, 5, 4, 3, and 1. As can be seen, the elegant organization of the basins is determined by the saddle order $3 \leq 4 \leq 5 \leq 6 \leq 1$ and can be summarized in the form

$$(6+(5+(4+(3+1)))) ,$$

with $\cdots p+(U)\cdots$ indicating "the set U accumulates

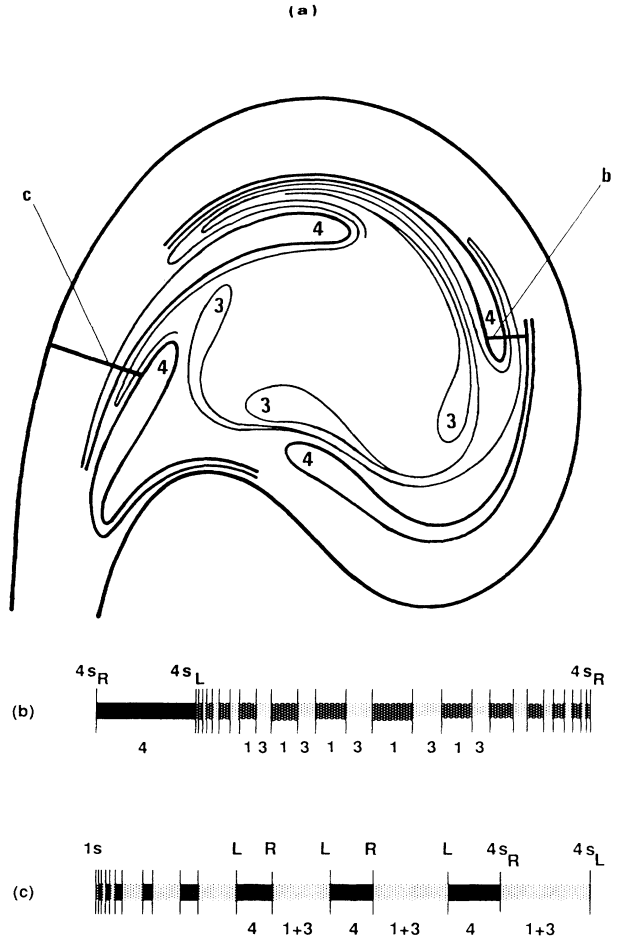

FIG. 8. (a) The basins of the period-3 and -4 orbits spiral outward in reverse iteration to accumulate on $1s$. However, when the period-3 basin passes "outside" a component of the period-4 basin, it "detours" to the "inside" of that component. This process is shown for just one of the components of the period-4 basin for clarity. In this way the period-3 basin accumulates on the period-4 basin while both accumulate on $1s$. (b) Intersections of the period-4, -3, and -1 basins with the line segment b have the structure shown. (c) Intersections of the period-4, -3, and -1 basins with the line segment c have the structure shown.

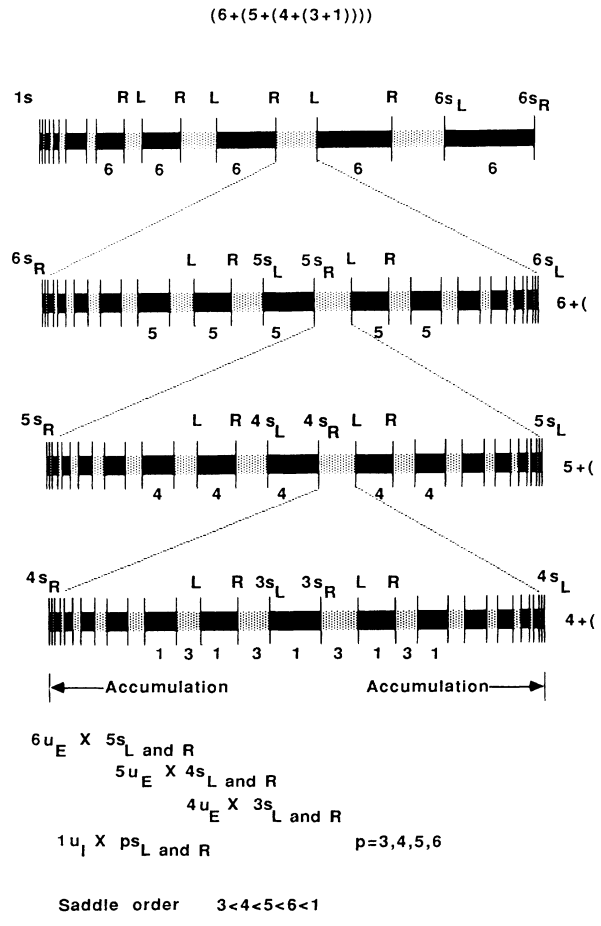

FIG. 9. Although coexisting basins of attraction are highly intertwined, there is simplicity in their complexity: the organization of the basins is determined by the order of the saddle crossings, or equivalently, by the saddle order.

on the period-p basin," and $(3+1)$ indicates the intertwining of the basins of the period-1 and -3 attractors.

This organizational structure allows us to resolve several of the questions raised in the Introduction. If a small ball of initial conditions near the period-1 saddle (or more generally near its inset) is allowed to evolve, the initial conditions will evolve into each of the coexisting basins with well-defined relative probability. For example, in the case

$$(6+(5+(4+(3+1))))$$

the initial conditions will evolve into the basins interior to the period-1 saddle with relative probability

$$P(6):P(5):P(4):P(3):P(1)\ . \tag{3.1}$$

The actual attractor in any of these basins may be a period-doubled version of the fundamental periodic orbit (e.g., 5×2^k) or may even be a chaotic attractor based on that branch. If a small ball of initial conditions exterior to one of the basins but near its saddle inset (for example, the period-4 saddle) is allowed to evolve, the only accessible final periodic orbits are within those basins bounded by the insets of the saddles interior to the period-4 saddle. Thus the final state lies within either the period-3 or the period-1 basin. Further, the relative probability for the final state to occur in these basins is $P(3):P(1)$, where the relative probabilities are those given in (3.1) for initial conditions near $1s$. In fact, the relative probabilities $P(3):P(1)$ can be determined by allowing initial conditions to evolve from the neighborhood of the inset of *any saddle exterior* to the period-3 saddle.

Conversely, suppose the system has a stable periodic orbit of period p and the period-p basin is destroyed by changing the control parameter. Following transients whose periodicities are given by all saddles interior to the period-p saddle, the system will settle into one of the interior basins. For example, if the basin organization is again

$$(6+(5+(4+(3+1))))$$

and the period-4 basin is destroyed by inverse saddle-node bifurcation,[9] only the interior basins of periods 3 and 1 will be occupied, and these with relative probabilities $P(3):P(1)$. These probabilities are precisely those determined in the preceding paragraph. This occurs because, except for the basin undergoing saddle-node bifurcation, the relative volume of each of the coexisting basins changes very slowly during the saddle-node bifurcation, as will be seen in Sec. IV. This behavior has been observed in recent experiments on the laser with modulated parameter.[19]

IV. BIRTH OF A BASIN

In this section we determine the effects of a saddle-node bifurcation on the organization of the basins of a dynamical system. This study includes a neighborhood of the control parameter space (R for the laser, a for the Henon map) containing the value at which the saddle-node bifurcation occurs. We will determine how the basins which are present before the saddle-node bifurcation takes place rearrange themselves as the critical control parameter value is approached, what occurs at the saddle-node bifurcation, and what takes place immediately after the saddle-node bifurcation.

We consider the occurrence of the saddle-node bifurcation within the context of Newhouse orbits. Incorporation of non-Newhouse orbits within this descriptive framework is possible once their saddle order is known. Organization of the non-Newhouse basins among the Newhouse basins is governed by crossing relations of the type (2.2), or equivalently, of their saddle ordering. For concreteness, we assume that the saddle-node bifurcation creates a period-4 basin in the presence of coexisting basins of periods 1, 3, 5, and 6. The basin organization after the saddle-node bifurcation is

$$(6+(5+(4+(3+1))))\ ,$$

indicated in Fig. 9. Before the saddle-node bifurcation, the basin organization is

$$(6+(5+(3+1)))\ ,$$

with analogous structure. It is clear that the saddle-node bifurcation forces the drastic rearrangement[20] of the basins "interior" to the period-4 basin: $(3+1)$. The period-4 basin is born accumulating on the "exterior" basins, $(6+(5))$, but does not force their rearrangement. In order to gain an understanding of the processes involved in the creation of a new basin by saddle-node bifurcation, it is therefore sufficient to consider only those basins interior to the basin being born.

As a result of these considerations, it is sufficient to consider the birth of the period-4 basin in the presence of only the coexisting period-3 and -1 basins. When the period-4 saddle-node bifurcation occurs, we have the following crossing relations:

$$\begin{aligned}
&\text{(i)} \quad 1u_I \times 3s_L \ \text{ and } 3s_R\ , \\
&\text{(ii)} \quad 1u_I \times 4s_L \ \text{ and } 4s_R\ , \ \text{New} \\
&\text{(iii)} \quad 4u_E \times 3s_L \ \text{ and } 3s_L\ , \ \text{New}\ .
\end{aligned} \tag{4.1}$$

The first relation requires that the period-1 and -3 basins accumulate on the boundary $1s$ of the attractor at infinity. It also requires that $1u_I$ accumulates on $3u$. This crossing, and its accumulation implications, is present before the period-4 saddle-node bifurcation.

The second crossing relation, new after the saddle-node bifurcation, requires that all three basins accumulate on $1s$ in the intertwined manner shown in Fig. 8. It also requires that $1u_I$ accumulates on $4u$.

The last crossing relation requires that $3s$ accumulate on $4s$ as well as $1s$.

The two new crossing relations requires that $3s$ accumulates on $4s$, and $1u$ accumulates on $4u$, at the moment of creation of these two new invariant sets. This requires a dramatic rearrangement of the invariant sets $3s$ and $1u$ leading up to the saddle-node bifurcation.

This rearrangement appears to take place in a canonical way. The canonical properties can be determined from a study of the properties of the fold catastrophe for a gradient dynamical system.[21] The fold catastrophe is il-

lustrated in Fig. 10. It should be noted that the basin of attraction is formed with nonzero volume at the saddle-node bifurcation [Fig. 10(a)]. After the saddle-node bifurcation, both the saddle and node have invariant sets. When the saddle and node become degenerate, the saddle inset becomes degenerate with one of the nodal insets [Fig. 10(b)]. Before the saddle-node bifurcation, these insets are no longer present as invariant sets.

There is, however, a natural decomposition of the flow into two complementary directions which is valid in a neighborhood of (before, during, after) the saddle-node bifurcation. This decomposition is easily constructed beginning at the saddle-node bifurcation. Linearization of the flow at the doubly degenerate critical point yields one zero eigenvalue and a nonzero eigenvalue. The center manifold passes through the degenerate critical point and is tangent to the eigenvector with vanishing eigenvalue. The flow direction corresponding to the eigenvector with nonzero eigenvalue is the contracting direction. Under perturbation, which splits the degenerate critical point into nondegenerate critical points, the center manifold evolves into the slow manifold. This consists of the outset of the saddle which feeds the node, together with the collinear invariant sets of the saddle (an outset) and the node (an inset). The contracting direction is determined by the eigenvectors of the saddle and node which have "large" eigenvalues, that is, which evolve continuously from the nonzero eigenvalue of the degenerate critical point. Under a perturbation of the degenerate critical point which causes the critical points to disappear, the slow manifold and contracting direction are the continuations of the center manifold and the contracting direction of the degenerate critical point. This decomposition is illustrated in Fig. 10. The center manifold is the horizontal axis ($a=0$), the slow manifold is its continuation ($a<0$, $a>0$), also the horizontal axis. The contracting direction is the vertical axis in all three cases. A more precise definition of slow and center manifolds is the following: The center manifold is associated with the eigenvalues with zero real part in the linearization of a flow around a fixed point.[13] In the study of the bifurcations at $\mu=0$ of $dx/dt=f(x,\mu)$ around $x=0$ it is convenient to reduce the flow to the center manifold of the augmented set of equations in phase *and* control parameter space[22] $dx/dt=f(x,\mu)$, $d\mu/dt=0$. The slow manifold of the original equation $dx/dt=f(x,\mu)$ is the intersection of the center manifold of this augmented set of equations with planes of constant control parameter value $\mu=\mu_0$.

These properties of a gradient dynamical system apply to the saddle-node bifurcations for the systems (1.1) and (1.2), and can be used to determine the canonical properties in the neighborhood of a saddle-node bifurcation. It is possible to determine how $3s$ approaches the impending accumulation point in this slow manifold as the saddle-node bifurcation is approached. To this end, we let x measure the distance from the critical point centroid

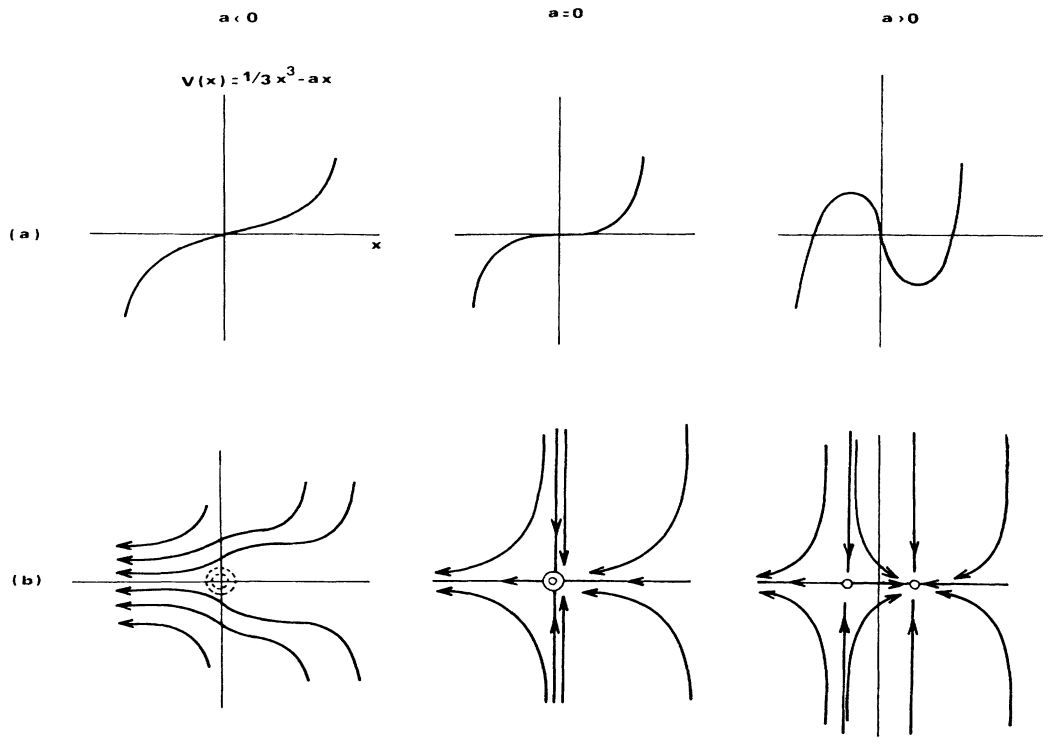

FIG. 10. (a) The fold catastrophe, $A_2(x)=\frac{1}{3}x^3-ax$, has the canonical form shown. The saddle-node bifurcation occurs at $a=0$. Immediately following the saddle-node bifurcation the basin of attraction, which is the set of x with $-\sqrt{a}<x$, has nonzero volume. (b) Flows $dx_i/dt=-\partial V/\partial x_i$ have the form shown for the potential $V(x_1,x_2)=A_2(x_1)+\frac{1}{2}x_2^2$. Degenerate saddle and node insets ($x_1=0$) are created at $a=0$. The slow manifold is the line $x_2=0$.

along this slow manifold. Then intersections of $3s$ with this slow manifold are governed by the canonical equation for the fold catastrophe[21]

$$dx/dt = -\text{grad}V \ , \tag{4.2}$$

where $V(x)$ has the canonical form of a fold catastrophe: $V(x)=x^3/3-ax$. By integrating this equation through one period T from a fixed initial condition x_0 in phase space, we can determine the location of successive intersections of $3s$ with the invariant set. The nth intersection with the slow manifold is

$$\begin{aligned} x_n &= [x_0 - \sqrt{-a}\,\tan(\sqrt{-a}\,nT)]/[1+(x_0/\sqrt{-a}\,)\tan(\sqrt{-a}\,nT)] \quad (a<0) \ , \\ x_n &= [(1/x_0)+nT]^{-1} \quad (a=0) \ , \\ x_n - \sqrt{a} &= (2\sqrt{a}\,)/[(x_0+\sqrt{a}\,)/(x_0-\sqrt{a}\,)(\lambda)^n - 1] \quad (a>0) \ , \end{aligned} \tag{4.3}$$

where $\lambda=\exp(2aT)$. The results are illustrated in Fig. 11.

This figure conveys the following information. Before the saddle-node bifurcation ($a<0$), successive intersections of the inset $3s$ with the slow manifold slow down in the neighborhood of the (complex) critical points, with the minimum separation between successive intersections governed by the imaginary part of the virtual saddle-node pair,

$$\Delta x_{\min} = (-a)T = |x_c - x_c^*|^2 T/4 \ .$$

Thus passage of the period-3 saddle inset through the neighborhood of the impending period-4 saddle-node bifurcation contains information about the location of this bifurcation in both phase space (symmetry axis) and in control space (minimum separation). At the degenerate critical point ($a=0$), the approach is arithmetic, going asymptotically like $1/n$. After the saddle-node bifurcation ($a>0$), the inset $3s$ approaches the nondegenerate saddle along the saddle outset geometrically at the rate $(1/\lambda)^n$, where λ is the eigenvalue of the period-4 saddle outset.

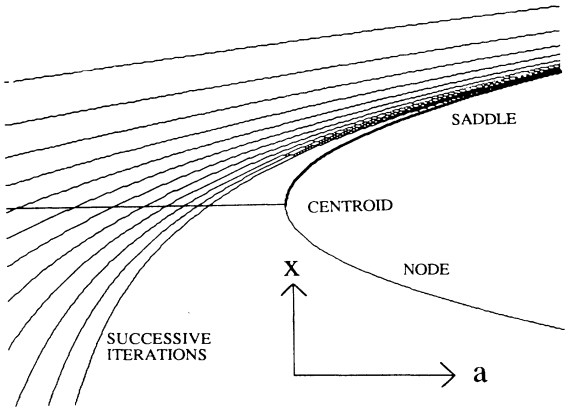

FIG. 11. Starting from an initial condition, x_0, successive inverse iterations ($a>0$) approach the saddle along the slow manifold (at this point it is the saddle outset) geometrically with a rate $(1/\lambda)^n \sim e^{-n(2aT)}$, arithmetically ($a=0$) at a rate $\sim 1/n$, or ($a<0$) fail to accumulate in this region, passing through the neighborhood of the centroid with minimum step size bounded below by $\Delta x_{\min} = (-a)T = |x_c - x_c^*|^2 T/4$.

The reorganization of the manifolds $3s$ and $1u$ in the neighborhood of the period-4 saddle-node bifurcation is illustrated in Fig. 12. As the period-3 basin components (or $3s$) spiral outward toward the boundary of infinity, they must "detour" to enclose and accumulate on the period-4 basins. Before the period-4 saddle-node bifurcation these approach, but do not accumulate on, the impending period-4 structures. As the saddle-node bifurca-

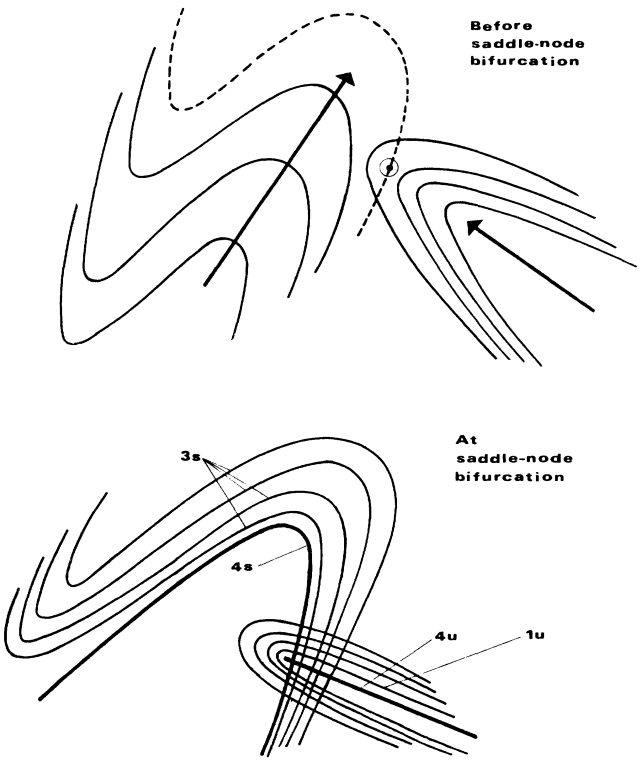

FIG. 12. (a) As the saddle-node bifurcation approaches, the invariant set $3s$ becomes increasingly distorted in the neighborhood of the impending period-4 basin, appearing to be expelled from this region (upward arrow). The invariant set $1u$ is also preparing to accumulate on $4u$ (leftward arrow) the moment it is formed. (b) At the saddle-node bifurcation, $3s$ accumulates on $4s$ and $1u_I$ on $4u_E$, as shown.

tion approaches, the invariant manifolds $3s$ are "expelled" from the regions in which the period-4 basins will be formed, as shown by the arrow in Fig. 12. At the same time, increasing numbers of folds of $1u$ approach the impending period-4 saddle-node bifurcation, as shown by the other arrow in Fig. 12. The region in which the period-4 basin is about to be born is one of very long transients, with the duration of the transients increasing as the critical value for saddle-node bifurcation is approached. At saddle-node bifurcation, $3s$ accumulates on $4s$, which has just come into existence, and $1u$ accumulates on that part of the slow manifold which has become the period-4 saddle outset. The period-4 basin is born with nonzero measure. Beyond the saddle-node bifurcation, the node moves from the boundary of the period-4 basin into the interior of the basin in the direction of the component of $4s$ which has locally the maximum curvature, as shown in Fig. 3.

V. EVOLUTION OF A BASIN

In this section we describe the evolution of a basin of attraction between its birth in a saddle-node bifurcation and the onset of its disintegration in a homoclinic tangency. As aging progresses, the basin boundary becomes increasingly wrinkled. A principal result is that the strips of basins shown as solid regions in Figs. 7 and 8 are not solid at all. Rather, the boundary becomes so folded it appears that "fingers" of the complementary basins are inserted into the original basin. These fingers become so numerous as homoclinic tangency is approached that they also accumulate. This increasing wrinkling occurs in a systematic way.

There are at least four mechanisms responsible for the increasing distortion of a basin boundary during this stage of the evolution of a basin. In the context of Newhouse basins, for a basin of period p the following are the crossings:

$$\begin{aligned}
&(1)\ \ 1u_I \times ps_L \ \text{ and } ps_R\ , \\
&(2)\ \ p'u_I \times ps_L \ \text{ and } ps_R \ \ (p'>p)\ , \\
&(3)\ \ pu_I \times ps_L \ \text{ or } ps_R \ \ \text{(homoclinic crossing)}\ , \\
&(4)\ \ pu_I \times p's_R \ \text{ or } p's_L \ \ (p'>p)\ .
\end{aligned} \tag{5.1}$$

These mechanisms are listed in the order of increasing complexity in the sense that (4) implies (3) which implies (2) which in turn implies (1). The organizational hierarchy of the basins is a direct consequence of the crossings (2.1), (2.2), and (5.1). The manifestations of these crossings have characteristics which are common to all systems as well as features which change from system to system. We concentrate on these characteristics which are common to all systems.

A. Mechanism (1)

The crossing $1u_I \times ps_L$ and ps_R occurs at the moment the period-p basin is created in a saddle-node bifurcation. The crossing of $1u_I$ with both ps_L and ps_R means that the period-p basin accumulates on $1s$, as discussed in Sec. III. In Fig. 13(a) we illustrate the crossing $1u_I \times 4s_L$ and $4s_R$. The intersection of $1u_I$ with the inset $4s_L$ of basin component A occurs at a, while $1u_I$ intersects $4s_R$ at b.

Additional heteroclinic crossings of the type $1u_I \times ps_L$ or $1u_I \times ps_R$ occur as the basin evolves. These additional heteroclinic crossings of one or the other period-p saddle inset with $1u_I$ are associated with increased wrinkling of the period-p basin. These additional heteroclinic crossings occur in pairs involving the same branch (L or R), in contrast with the original crossings which involve one (or odd) crossing with each of the two saddle insets. In Fig. 13(b) we illustrate the heteroclinic crossing of $1u_I$ with the component $4s_L$ of the same basin component A, which occurs at c and d. Additional heteroclinic crossings of ps_L or ps_R result in increased wrinkling of the period-p basin boundary and insertion of fingers of other basins into a component of the period-p basin, as illustrated in Fig. 13(c). These figures include also other components of the period-p basin.

In the context of the approaching homoclinic tangency $1u \times 1s$, this mechanism is responsible for folding the four disconnected components of the period-4 basin into each other. A global view reveals the connectivity of the four components of the period-4 basin as well as that of the period-$(1+3)$ basin. However, the basins become so narrow that their structure is not apparent except under high magnification associated with a local view. Under such conditions it appears that fingers of the period-$(1+3)$ basin are injected into the period-4 basin. Local organization of the basins of coexisting period-$[4+(3+1)]$ attractors is illustrated in Fig. 14. The four components $A4$, $B4$, $C4$, and $D4$ are intertwined and separated by strips of period-1 and -3 basins (components $A3$, $B3$, and $C3$ of the period-3 basin are similarly intertwined) separating the period-4 segments and accumulating on $4s$. The effect of folding the four basins into each other is illustrated in Fig. 15.

B. Mechanism (2)

The crossing $p'u_I \times ps_L$ and ps_R $(p'>p)$ occurs at the moment either is created in the presence of the other. These crossings require the period-p basin to accumulate on the period-p' basin, and both to accumulate on $1s$, as described in Sec. III. In addition, it is possible for one of the insets ps_L or ps_R to have additional pairs of heteroclinic intersections with $p'u_I$. The remarks made above (for the period-p basin) about the wrinkling and insertion of fingers of other basins required by the crossings $1u_I \times ps_L$ or ps_R now apply, *mutatis mutandis*, to the period-p basin forced by the crossings $p'u_I \times ps_L$ or ps_R.

C. Mechanism (3)

As the homoclinic tangency $1u \times 1s$ approaches, each Newhouse orbit formed in this process is forced into its own homoclinic tangency: $pu \times ps$. The evolution of one component of the period-p basis is shown in Fig. 16. The basin is shown at the instant of its creation in Fig. 16(a). As it evolves, the saddle and node separate in the canonical way, as shown in Fig. 16(b). The node moves in the direction of the more highly curved saddle insets: ps_c [for

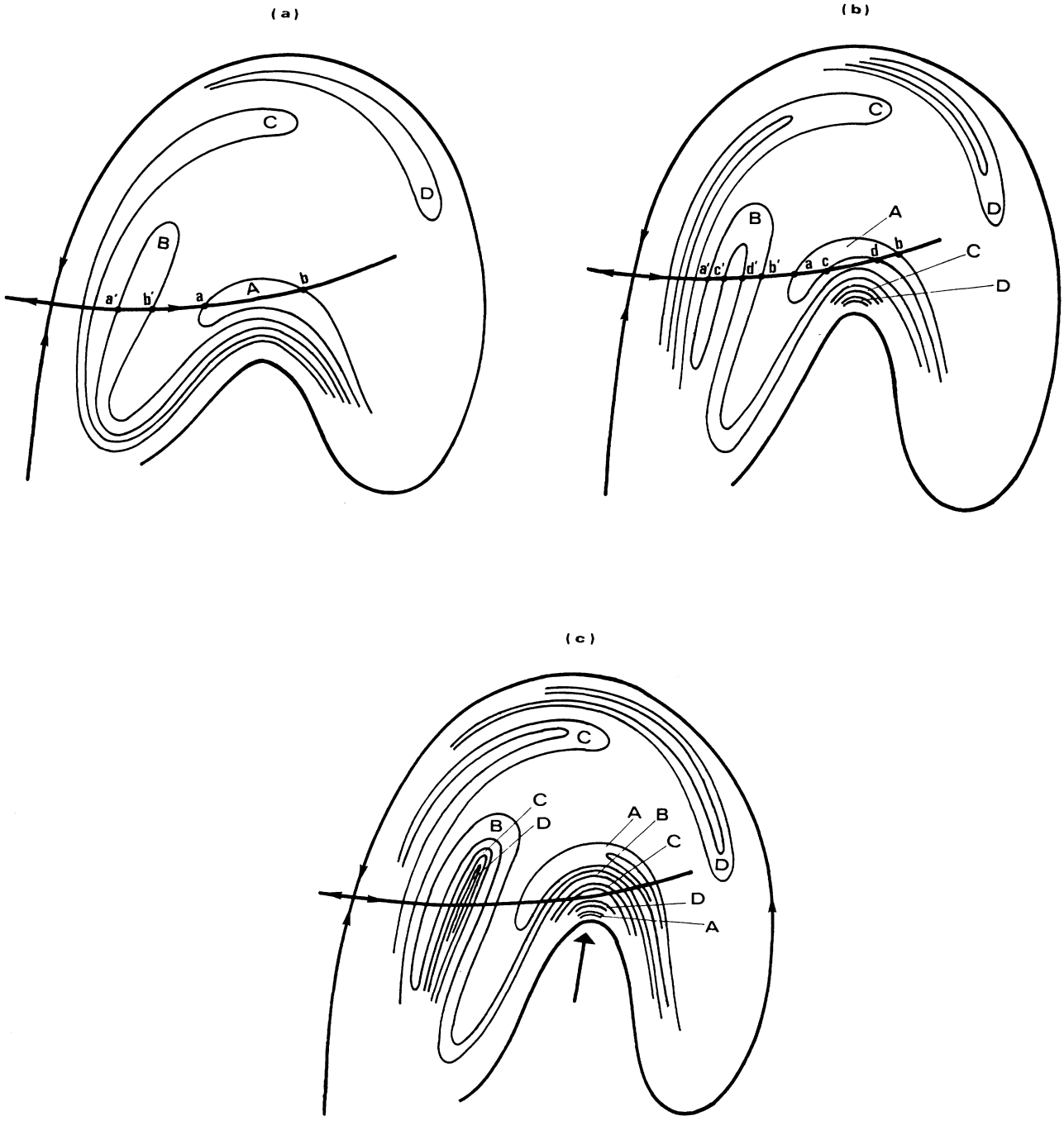

FIG. 13. (a) If component A of the period-4 basin of attraction has intersections at a,b with $1u$ near the period-4 saddle-node pair, then its preimage, component B, has intersections at a',b'. (b) As homoclinic tangency $1u \times 1s$ approaches, one inset of the period-4 saddle, $4s_c$, is "pushed across" $1u$, creating a pair of additional intersections at c,d. Their preimages at c',d' create a period-$(1+3)$ "finger" in component B, and their preimages c'',d'' create an even more elongated finger in component C. (c) As the approach to homoclinic tangency $1u \times 1s$ continues, strips from the other components B, C, D, A, . . . are pushed across $1u$, as indicated by the arrow. These crossings are responsible for "intertwining" the four components of the period-4 basin among themselves. The high degree of intertwining appears as the insertion of alternating fingers of period-4 basin and intertwined period-$(1+3)$ basins "within" the period-4 basin. As the homoclinic tangency $1u \times 1s$ approaches, an increasing number of strips of the period-4 basin cross $1u$ in the neighborhood of the "head" of component A. Components B, C, and D have similar structure. As a result, the four components become increasingly entangled.

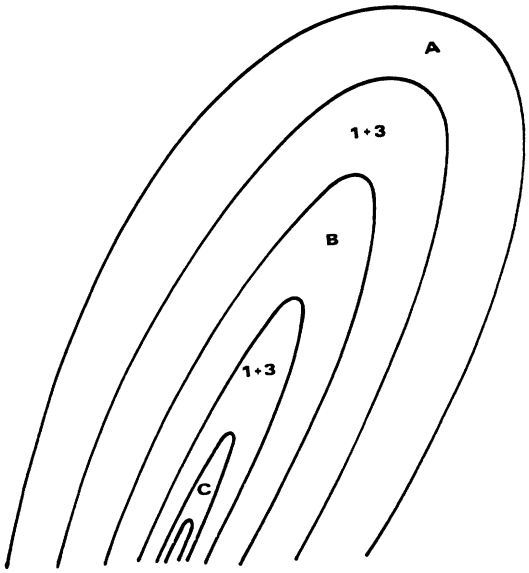

FIG. 14. General local organization of the components of the period-4 basin.

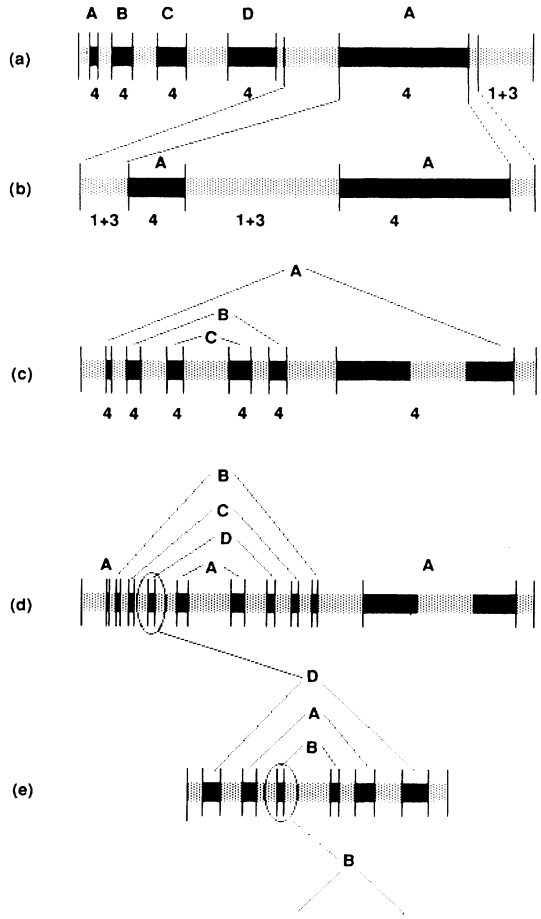

FIG. 15. The intersection of the intertwined basins (4+(3+1)) with a line [see, for example, Fig. 13(a)] has increasing complexity, as the homoclinic tangency $1u \times 1s$ approaches. Here (a)–(c) correspond to Figs. 13(a)–13(c). The general structure is shown in (d). Each of the strips may itself be "fingered" (e). If so, the structure shows the canonical organization indicated in (a). Inserted fingers may intersect the line more than once; each successive intersection occurs closer to the other component of the saddle inset.

the Henon map (1.2) $ps_c = ps_L$; the other, straighter saddle inset is labeled ps_s (straight)]. Initially, pu_I terminates on the stable node. Its curvature is associated with the period-doubling cascade which this node undergoes on the way to homoclinic tangency, $pu_I \times ps_c$. It is the component ps_c which becomes wrinkled as the homoclinic tangency $pu_I \times ps_c$ approaches.

As pu_I approaches ps_c, both become increasingly distorted, as shown in Fig. 16(c). At this stage, the basin exhibits a characteristic "dragonfin" profile. During the approach to homoclinic tangency a new sequence of "Newhouse orbits" is generated. These have period $p \times p'$, $p' \geq 3$ within the initial Newhouse basin of period p. At homoclinic tangency there are several kinds of accumulation. These are shown in Fig. 16(d). The inset ps_c accumulates on ps_s. The outset pu_I accumulates on itself. The outset pu_E does not participate in these accumulations. In addition, the secondary Newhouse orbits of period $p \times p'$ accumulate ($p' \to \infty$) onto ps_c within the fingers of pu_I, as well as into the period-p regular saddle. Further, the insets and outsets of these secondary Newhouse saddles accumulate on the inset and outset of the initial Newhouse saddle of period p.

The effect of the homoclinic tangency $4s \times 4u_I$ on the period-4 basin is illustrated in Fig. 17. As in Fig. 8, this represents the intersection of the period-(1+3) and -4 basins with a line segment. As this homoclinic tangency approaches, one component of the saddle inset becomes increasingly distorted, so that increasing numbers of intersections of the (1+3) basin and the same component of the period-4 basin occur. This progression is shown in Figs. 17(a)–17(f). The component of $4s$ which becomes distorted in this process is the same component of $4s$ which is distorted in the process described above and illustrated in Fig. 16. However, in this process the "inserted" fingers do accumulate on the other component of $4s$ at the homoclinic tangency $4s \times 4u$. As this tangency approaches, many (secondary) Newhouse and non-Newhouse orbits are created in the period-4 basin. All these basins accumulate on $4s$. They are not explicitly shown in Fig. 17, as their presence is not important for the ensuing discussion of how the period-4 basin is destroyed following the homoclinic tangency $4s \times 4u$. However, the saddles created in these bifurcations play a very important role in the disintegration of the basin after homoclinic tangency. It should be borne in mind that the processes generated by the crossing $1u \times ps$ and $pu \times ps$ occur simultaneously, so that the folding and intertwining of basins can appear extremely complicated, as suggested in Fig. 17(b), even when no more than two basins coexist.

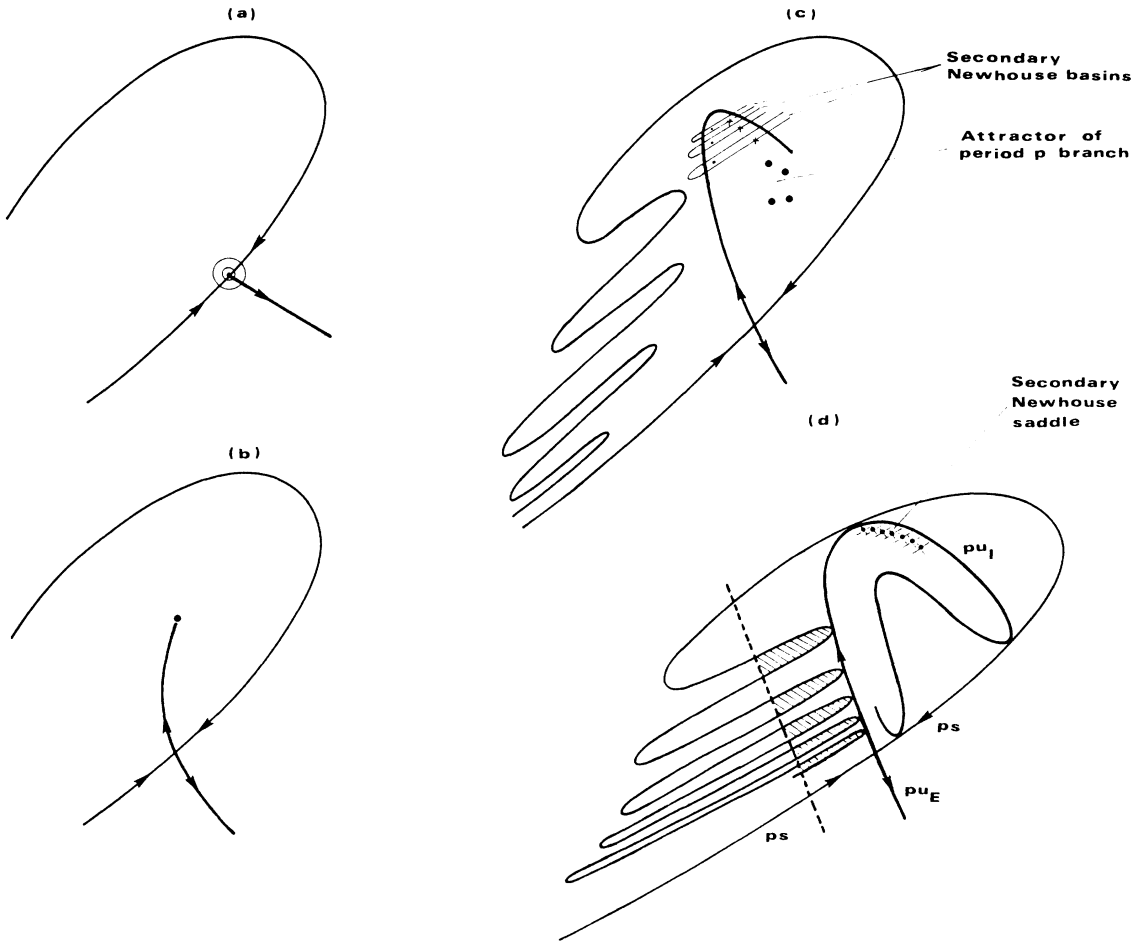

FIG. 16. Each Newhouse orbit undergoes its own homoclinic tangency before the homoclinic tangency ($1u \times 1s$), responsible for its birth, occurs. (a) Basin at birth. (b) The saddle and node move away from each other with canonical half-power-law dependence in the neighborhood of the saddle-node bifurcation. (c) As its homoclinic tangency $4s_c \times 4u_I$ approaches, the basin assumes a canonical "dragonfin" appearance, with $4s_c$ and $4u_I$ becoming increasingly distorted. A sequence of secondary Newhouse orbits of period $4 \times p'$ ($p' \geq 3$) is born within the period-4 basin. (d) At homoclinic tangency, $4s_c$ accumulates on $4s_s$ and $4u_I$ accumulates on itself. All secondary Newhouse basins of period $4 \times p'$ have been destroyed, leaving behind only the secondary Newhouse saddles of period $4 \times p'$ (shown) and a constellation of flip saddles (not shown). Secondary non-Newhouse basins and orbits may exist but are not shown. Hatching indicates coexisting basins of periods $(1+3)$ as well as strips of other components of the period-4 basin.

D. Mechanism (4)

The crossing $pu \times p's$ typically occurs after the period-p basin has disintegrated. This crossing would be responsible for further very complicated contortions of the basin, should it still exist. These further distortions have not been fully analyzed.

VI. DEATH OF A BASIN

Extensive wrinkling of the boundary of a basin is a sign of its old age, a prelude to its impending death. The death of a basin begins at homoclinic tangency and concludes with a crisis.[15,16,23] Many of the events which happen during this interval occur in a standard way. In this section we discuss the disintegration of a basin, which begins with homoclinic tangency. For specificity, this discussion is carried out for the basin of period 4.

At the homoclinic tangency, the fingers of $4s_L$ are lined up along $4u_I$, with the "tips" of the fingers making nongeneric (parabolic) contact with $4u_I$ [cf. Fig. 16(d)]. At homoclinic tangency, $4s_L$ accumulates on $4s_R$. Before tangency, $4s_L$ does not accumulate on $4s_R$; after tangency it accumulates on both $4s_R$ and $4s_L$.

As homoclinic tangency is passed, the fingers of $4s_L$ poke through $4u_I$. The nearer the finger passes to the period-4 saddle, the longer and thinner it is. Since $4s_L$

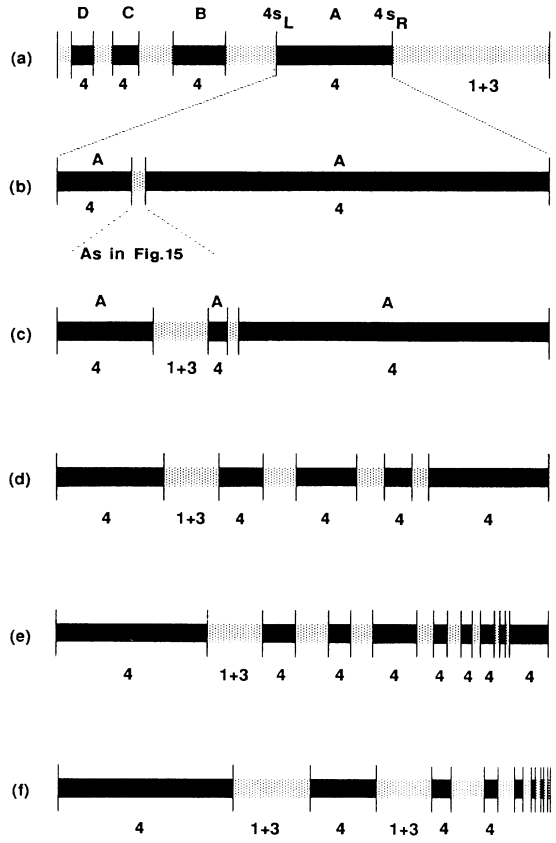

FIG. 17. The intersection of the line segment shown in Fig. 16(d) with component A of the period-4 basin is shown. The sequence progresses from its birth in a saddle-node bifurcation (a), through increasing distortion caused by the impending homoclinic tangency $4u \times 4s$ (b)–(e), to homoclinic tangency (f), at which $4s_c$ accumulates on $4s_s$. The basin between successive "fins of the dragon" is not simply the intertwined basin $(1+3)$, but includes also strips from other components of the period-4 basin, as indicated in (b).

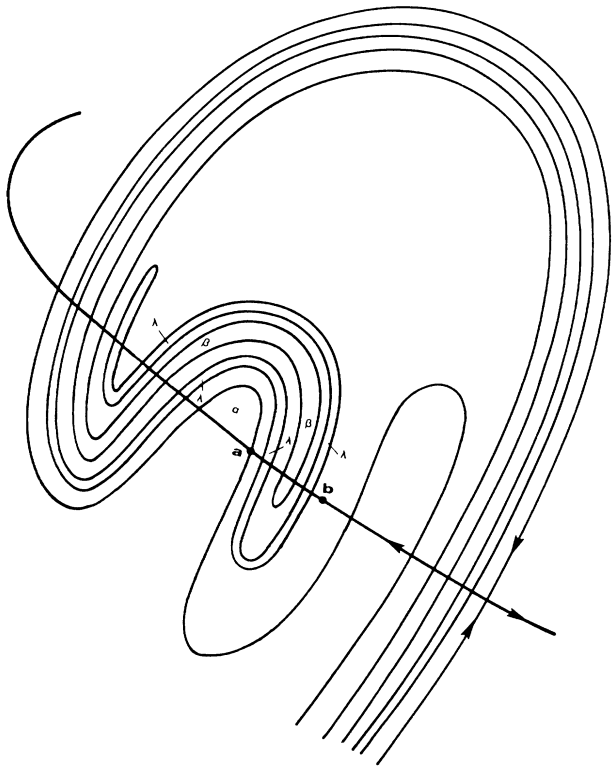

FIG. 18. After homoclinic tangency, the inset ps_L accumulates on itself. Long thin fingers poke through pu_I into the region formerly occupied by the period-p basin. Longer and thinner fingers wrap around the shorter fingers, *ad infinitum*.

accumulates on itself, every neighborhood of a point in $4s_L$ has nonempty intersection with other fingers of $4s_L$. That is, accumulating on a point in any finger of $4s_L$ are longer and thinner fingers of $4s_L$. The nature of this accumulation is shown in Fig. 18. Thinner fingers wrap around fatter fingers. This structure forces the intertwining of basins of periods 4 and $(3+1)$ in a complicated and organized way, as shown in Fig. 17. The result is that the intersection of $4u_I$ with $4s_L$ has the structure of a Cantor set. In short, the boundary of the period-4 basin has become so wrinkled that it has a fractal structure.[16,24,25] We define a boundary to be strange if it includes an invariant Cantor set. In this sense, a basin boundary can be strange even if there is no other attractor present. For example, if the remnants of a strange attractor after its death in a boundary crisis are immersed in a second basin of attraction, the boundary will be strange, since there are unstable Cantor sets which are limit sets of points in the basin.

Two of the accumulation points in this Cantor set can easily be identified. The exterior accumulation points (a in Fig. 19) in the Cantor set in the neighborhood of any finger are the intersections of the finger of $4s_L$ with $4u_I$. The interior accumulation points (b) are more interesting. Through these points passes a limiting curve which is, in a rough sense, the "exterior" boundary of the period-4 basin. To make this notion more precise, we note that a series of secondary Newhouse saddles ($4 \times p$, $p \geq 3$) exists within the period-4 basin and accumulates on $4s_L$ at homoclinic tangency. These secondary Newhouse saddles have an ordering identical to the ordering of the primary Newhouse saddles. Furthermore, the heteroclinic connections to increasing periodicity (2.3) are all satisfied; the heteroclinic connections $4(p+1)s \times 4pu$ to decreasing periodicity are also all satisfied down to some minimum value of p, p_0. All secondary Newhouse saddles $4p$ ($p \geq p_0$) are thus joined in a heteroclinic tangle.[13,15] This means that the insets and outsets of each accumulate on all the others in this cycle.

Immediately following homoclinic tangency, $4s_L$ accumulates on itself from inside the region of the period-4 basin. This requires fingers of $4s_L$ to pass through the series of secondary Newhouse saddles which accumulates on $4s_L$. These fingers of $4s_L$ must intersect the unstable manifolds of some secondary Newhouse saddles, $4pu$, for

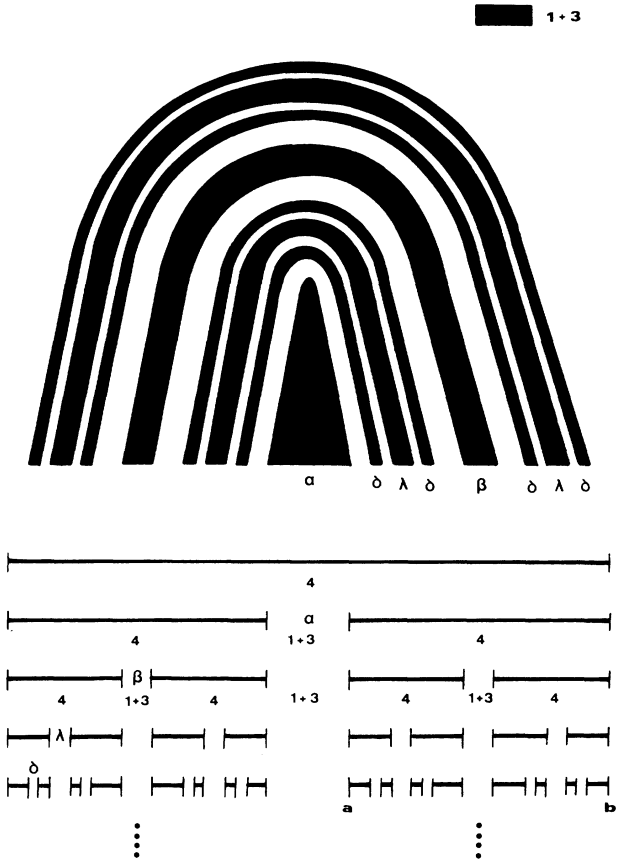

FIG. 19. The intersection of the inset ps_L with pu_I has the structure of a Cantor set. The points a and b correspond to a and b in Fig. 18. Top shows structure of the fingers of the complement C of the period-p basin in the neighborhood of the points a and b. Complement C consists of all basins "interior" to p, organized as shown in Fig. 9. Bottom shows steps in construction of the intersection of ps_L with pu_I obtained by removal of increasingly elongated fingers $\alpha, \beta, \gamma, \delta, \ldots$, of C. This construction clearly indicates the existence of a Cantor set in a transverse section of the period-p basin boundary.

p sufficiently large. Since all insets of the secondary Newhouse saddles intersect $4u_I$, the period-4 saddle also belongs to the heteroclinic tangle of secondary Newhouse saddles $4p$ ($p \geq p_0$). Therefore $4s_L$ must accumulate on $4ps$ for each secondary Newhouse saddle in the heteroclinic tangle. Since the lowest periodic orbit among these secondary Newhouse saddles is the "most interior" orbit, the interior limit points (b in Fig. 19) of the Cantor set are the intersections of $(4p_0)s$ with $4u_I$. In somewhat different terminology, the most interior saddle, $4p_0$, in this heteroclinic tangle is the saddle accessible from the interior of the period-4 basin.[15,16,26,27] (A saddle is accessible from a basin on one side of the stable manifold if and only if there exists a one-sided neighborhood of the saddle that belongs to the basin of attraction, with the only exception being those points belonging to the stable manifold itself. This concept was introduced by Grebogi and co-workers[26,27] and formalized in a different way using ideas of path continuity. A basin A is accessible from another basin B if the saddle whose inset bounds A is interior to the saddle whose inset bounds B.)

As the control parameter is further increased, additional heteroclinic connections, typically with the secondary Newhouse orbit of next lower periodicity (e.g., $4p'$, $p'=p_0-1$), may occur. When this happens, $4s_L$ accumulates on $(4p')s$, so that the interior of the basin boundary appears to make a sudden jump inward from the initial accumulation set $(4p_0)s$ to a more interior accumulation set, which is $(4p')s$.[15,16] The most interior of the secondary Newhouse saddles is $4p'$ with $p'=3$. Once this limit set is reached, there are no further small changes in the basin boundary due to more interior (secondary) Newhouse saddles, since there are none.

The process of upward closure [i.e., saddle connections $4(p+1)s \times 4pu$, with decreasing period] of the secondary Newhouse orbits is responsible for the increasing disintegration of the period-4 basin. Death or expansion of the (strange) attractor comes about when the attractor touchs the basin boundary in a crisis. Which one occurs depends upon the nature of the boundary.[28]

When an attractor A collides with the common boundary of the basins of A and B, the attractor A is destroyed. The neighborhood of the former attractor A is embedded in the basin of B. In the place of attractor A are long-time chaotic transients. We call a region of chaotic transients a zone in phase space that contains transients of any time length and the limit of these transients is an unstable-invariant Cantor set. These transients mimic the periodicities present in this region just prior to the crisis. That is, for the period-4 basin the transients are of periods 4, 3, 1 [or period-doubled versions, neglecting all secondary (non-)Newhouse basins]. This process is illustrated in Fig. 20 in the case of the death of the period-4 strange attractor in the presence of the period-3 and -1 attractors for the Hénon map.

When attractor A reaches a strange boundary (for example, a region of chaotic transients) it expands into it and generates a new strange attractor that visits both the former region of transients and the region previously visited by A. This process has been reported for the laser system in theoretical work.[9,10]

VII. ADDITIONAL STRUCTURES

While each period-p basin evolves, the attractor within the basin also evolves. Typically, the attractor undergoes a period-doubling cascade. This cascade induces a further refinement in the basin structure. This refinement is illustrated in Fig. 21. After the first period doubling, each of the p components of the period-p basin is split in two by the inset of the period-p flip saddle [Fig. 21(a)]. Each half of a period-p component is mapped into the other by the pth iterate of the map. Following a second period doubling, each of the p components is divided into four parts by the period-p and -$2p$ flip saddles [Fig. 21(b)].

Another circumstance which induces modifications in the basin structure is the phenomenon of snaking.[29] This occurs when a branch undergoes one or more inverse

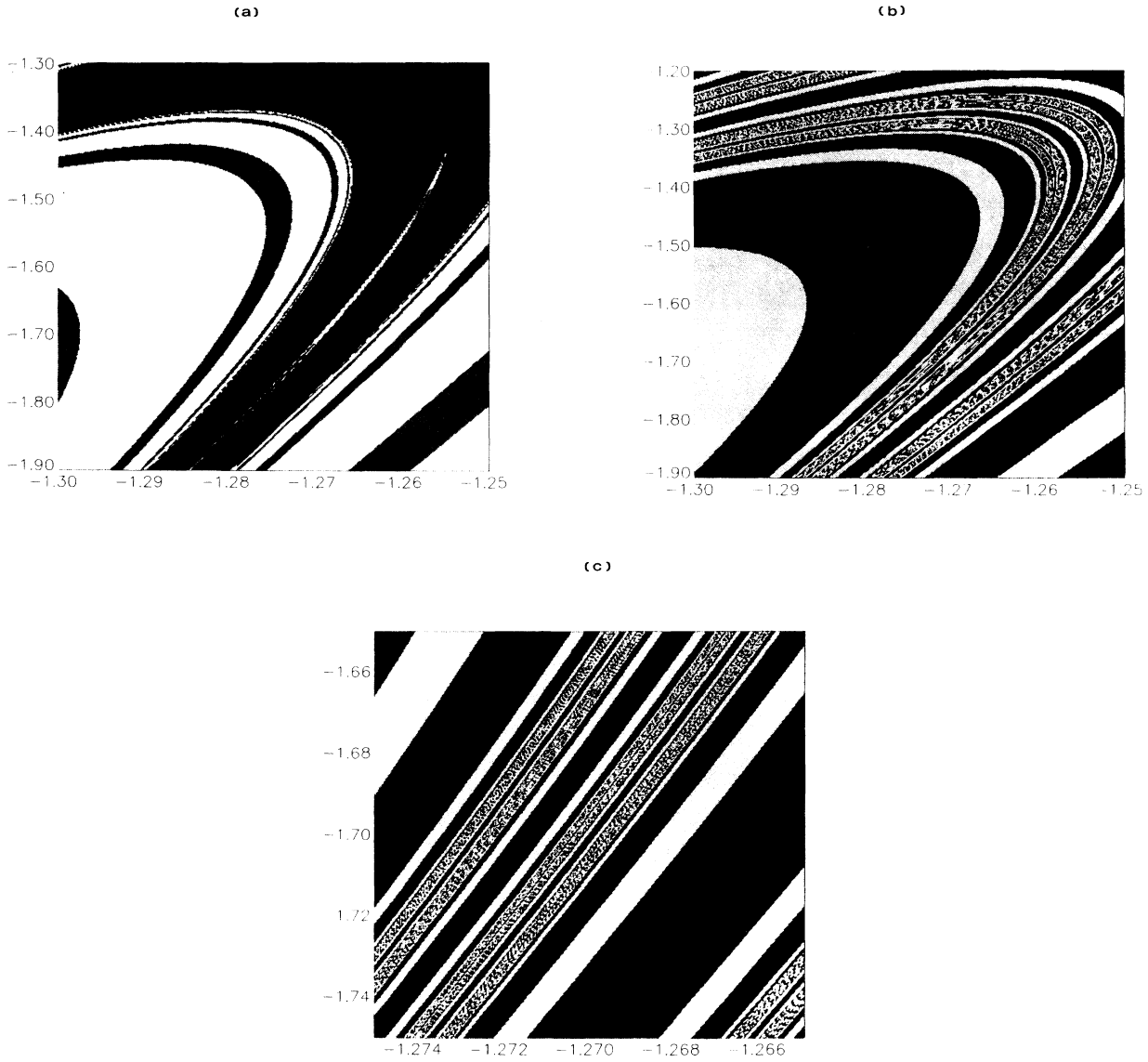

FIG. 20. Coexisting basins of attraction of the Henon map for $J=0.35$. (a) For $a=1.135$ there are three coexisting basins of period-1 (light), -3 (medium), and -4 (dark). (b) For $a=1.15$ the period-4 basin has disappeared, leaving in its place highly intertwined period-1 and -3 basins. (c) Enlargement of (b), showing intertwining of period-1 and -3 basins at an ever finer level.

saddle-node bifurcations, as illustrated in Fig. 22(a). This can occur in two ways, one involving a bubble diagram, or isola (not shown), the other as indicated in Fig. 22(a). The topological constraint on the snaking process is that all critical points belonging to the same branch lie on the same invariant set and satisfy the usual index theorems. The snaking phenomenon is governed by a cuspoid catastrophe along this invariant set.[21] This means in practice that the saddles and nodes must alternate along the invariant set, as shown in Figs. 22(b)–22(e). Any organization consistent with these constraints is feasible (e.g., multiple snakes). The snake illustrated in Fig. 22(a) is related to the A_3 (cusp) catastrophe, as seen by rotating Fig. 22(a) counterclockwise by 90°.

When the dynamics of a system is governed by a horseshoe there are no regular saddles of period 2 and only one each of periods 3 and 4 when the horseshoe is completed. Therefore if a period-2 saddle-node bifurcation is observed, it must be connected by a snake to the period-doubled orbit from the period-1 branch. If two or more saddle-node bifurcations of period 3 occur, they must be related by a snake, and similarly for period 4.[11]

VIII. SUMMARY AND CONCLUSIONS

We have studied the structure of the basins of attraction for coexisting Newhouse attractors. This discussion is based on the heteroclinic structure that is common to

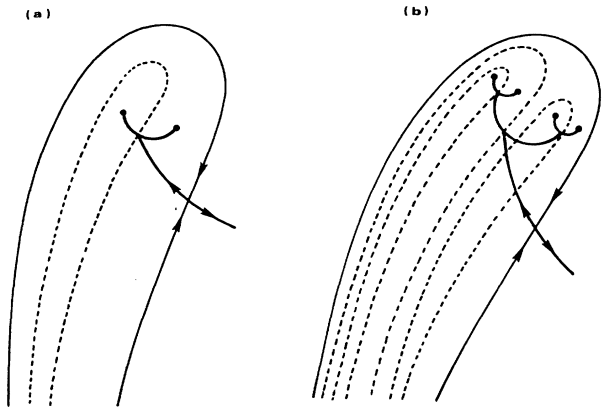

FIG. 21. The structure of the basin of attraction along a period-p branch evolves as the attractor evolves. Each of the p components of the period $p \times 2^k$ attractor is partitioned into 2^k parts by the k flip saddles remaining after k period-doubling bifurcations. Dashed lines show the partition after the first (a) and second (b) period-doubling bifurcations.

the laser system and the Henon map. This organization is general for systems associated with horseshoe maps.

The basins for a flow or map are organized in a systematic way. When two or more basins coexist, their global organization is governed by the order of saddle crossings, given in (2.1) for the special class of Newhouse orbits. A single crossing requires a countable number of additional crossings. This in turn requires accumulation of insets on insets, outsets on outsets. Since saddle insets typically separate basins, the accumulation of a saddle inset on an invariant set implies the accumulation of the two basins (one on each side of the saddle inset) on that invariant set. The accumulation typically has the appearance of a series of alternating strips of decreasing thickness.

Speaking roughly but accurately, the basins spiral outward toward the boundary of the attractor at infinity in reverse iteration sequence. The order of saddle crossings determines an order for the basin organization, from "inside to outside." As an interior basin spirals outward; it encounters all basins exterior to it and accumulates on each. This builds up the intricate and elegant accumulation structure of multiple coexisting basins which is shown in Fig. 9.

As the control parameter changes and the homoclinic crossing $1u \times 1s$ approaches, each of the coexisting period-p basins becomes more and more convoluted. The basins undergo two kinds of distortions. Two distinct but correlated mechanisms are responsible for these two types of distortions.

The crossing $1u \times ps$ forces the p distinct components of the period-p basin to become more and more thoroughly intertwined as the homoclinic crossing $1u \times 1s$ is approached. The mechanism is discussed in Sec. III and illustrated in Fig. 13(c). The homoclinic crossing $1u \times 1s$ forces the homoclinic crossing $pu \times ps$. This crossing is responsible for the dramatic wrinkling of one of the two components of the period-p saddle inset

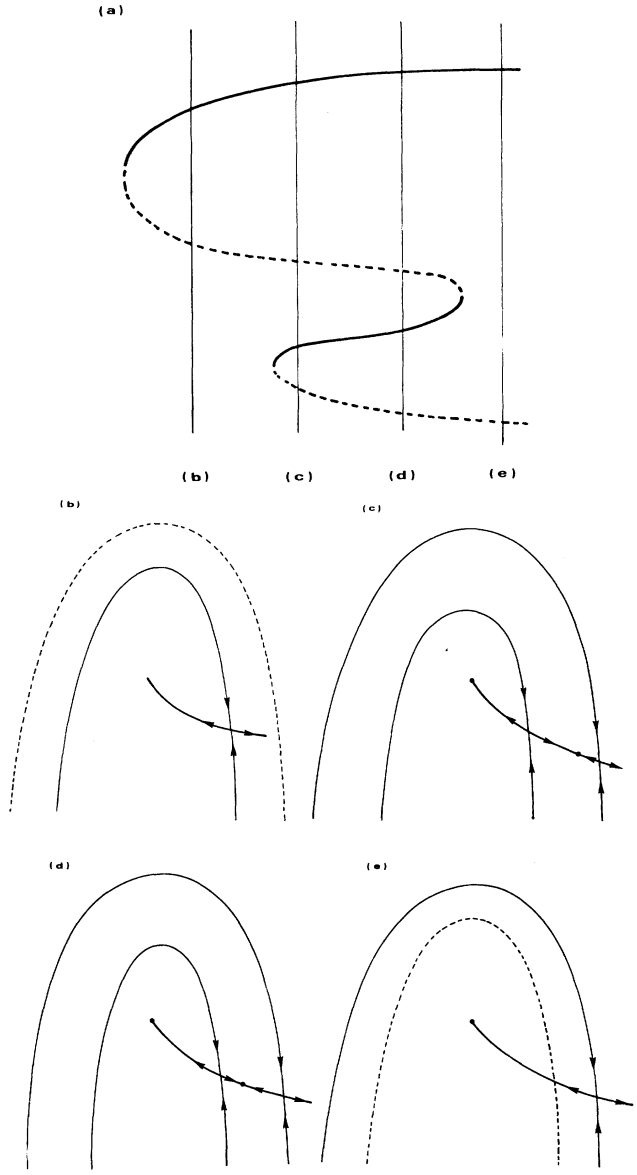

FIG. 22. (a) A period-p branch may undergo one (shown here) or more inverse saddle-node bifurcations. The structure of the basins of the stable components of the snaked branch is shown, for control parameter values (b)–(e), in parts (b)–(e) of this figure. (b) Only one stable period-p attractor is present, with boundary shown as solid curve. Location of boundary of second stable branch, which will appear between (b) and (c), is shown as dashed curve. (c) Two coexisting period-p basins are shown. Four critical points exist along the invariant set transverse to the basin boundaries: two nodes and two saddles. (d) As the control parameter increases, the intermediate node moves from the new saddle towards the original saddle. (e) Original saddle and new node have annihilated each other in an inverse saddle-node bifurcation. Location of original basin boundary is shown by dashed curve. Critical slowing down occurs in neighborhood of the dashed curves (virtual basin boundaries). For branches with multiple snakes, saddles and nodes are distributed along the invariant set transverse to the boundaries according to cuspoid catastrophes.

(ps_c), which exhibits the characteristic dragonfin shape. These two mechanisms, the one intertwining the components, the other wrinkling the components, occur in a highly correlated way. Both mechanisms are responsible for the "insertion of fingers" of the complementary basins into the period-p basin.

New basins are born into, and old basins removed from, this rigidly organized structure in a systematic way. New basins are introduced by saddle-node bifurcation. At birth, new basins have nonzero measure and are organized with respect to those basins already present in a way determined by their order of saddle crossings. As the birth of a basin approaches, insets of the interior saddles rapidly reorganize themselves so that accumulation on the new saddle insets will occur when these new saddle insets are born. This reorganization occurs in a canonical way which is described quantitatively by the fold catastrophe. This description is presented in Sec. V and illustrated in Figs. 11 and 12.

When a basin is born in a saddle-node bifurcation, its boundary is smooth and accumulates on all exterior basins (i.e., whose outset crosses the inset of the new saddle). In addition, its boundary is the accumulation of the insets of all coexisting interior saddles (i.e., whose insets cross the outset of the new saddle). As the control parameter increases, the basin and its attractor evolve. The attractor evolves through a period-doubling cascade which is correlated with, but not directly determined by, the evolution of the basin and its boundary. The basin becomes increasingly wrinkled and convoluted through the two mechanisms summarized above. This evolution is responsible for the insertion of fingers of lower period (more generally, interior) basins "into" higher-period (more generally, exterior) basins. In fact, such fingers are typically so narrow they can only be seen with high-resolution graphics, which precludes the global viewing necessary to identify the process as folding rather than "insertion." It should always be remembered that the saddle insets are two sided, with the associated basin on only one side and its complement on the other.

Disintegration and death come to a basin beginning with the homoclinic tangency of the regular saddle invariant sets. Just beyond homoclinic tangency the complement of the basin is mixed into its interior, accumulating on the former boundary from both sides. The thickness of this accumulating layer changes discontinuously as the invariant set ps crosses secondary Newhouse outsets $(p \times p')u$ of successively decreasing period, until the last (lowest) saddle outset has been crossed. At this point the next major change in the basin is its destruction in a crisis. Remaining after the destruction of the basin are the invariant sets of the regular period-p saddle, together with the invariant sets of the secondary Newhouse orbits. These measure-zero invariant sets govern transient behavior of the phase space in the neighborhood of the defunct attractor.

The order in which new attractors are born as a function of the parameters is known not to be canonical. In contrast, the organization of their manifolds, and with them, the organization of their basins of attraction, is canonical (at least for Newhouse attractors). This organization will manifest itself whenever two or more Newhouse saddles exist regardless of their periodicity. The fingerprints of their presence range from an accumulation process of basins onto basins to the existence of fractal boundaries between basins and regions of strange (fractal) transients.

As an additional example of this organization we can mention the Duffing oscillator. For that matter, any system resulting from adding dissipation and harmonic driving to a one-degree-of-freedom Hamiltonian system will present the heteroclinic structure given by (2.1) and (2.2). It can be shown that this structure results from the resonant bifurcations of the Hamiltonian orbits. This consideration puts a lower limit to the scope of this work.

The systematic organization of coexisting basins of attraction allows us to predict the behavior of the laser with modulated parameter, and other driven dynamical systems as well, when initial conditions are allowed to evolve to their final states. For initial conditions in the neighborhood of a period-p saddle inset but exterior to the basin of a period-p branch, the final state can occur in any accessible basin. Accessible basins are those basins bounded by saddles interior to the period-p saddle. The relative probability of occupation of the accessible basins can be determined by carrying out this experiment from the neighborhood of the period-p saddle inset or the inset of *any* saddle exterior to the period-p saddle. Such experiments have been done by initializing the system in the period-p basin and adding noise until the system is "bounced out" of that basin. They have also been done by changing the control parameter value until the period-p basin has been annihilated in an inverse saddle-node bifurcation. In both cases population of only those basins interior to the period-p basin (basins accessible from p) has been observed.[19]

In summary, basins evolve. They make their presence known before birth by a distortion created in the preexisting structures (cf. Fig. 12). Upon birth their surfaces are smooth. As they evolve their surfaces becomes increasingly wrinkled. After their death they leave reminders of their existence.

ACKNOWLEDGMENTS

We wish to thank Professor J. R. Tredicce, Professor P. Holmes, Professor K. T. Alligood, and Dr. J. Heagy for useful discussions. One of the authors (H.G.S.) wishes to thank Consejo Nacional de Investigaciones Cientificas y Tecnicas (CONICET) of Argentina. Support from National Science Foundation Grant Nos. PHY 84-51732 and PHY 85-20634 is gratefully acknowledged.

[1]F. T. Arecchi, R. Meucci, G. P. Puccioni, and J. R. Tredicce, Phys. Rev. Lett. **49**, 1217 (1982).
[2]R. S. Gioggia and N. B. Abraham, Phys. Rev. Lett. **51**, 650 (1983).
[3]F. T. Arecchi, G. L. Lippi, G. P. Puccioni, and J. R. Tredicce, Opt. Commun. **51**, 308 (1984).
[4]G. P. Puccioni, A. Poggi, W. Gadomski, J. R. Tredicce, and F. T. Arecchi, Phys. Rev. Lett. **55**, 339 (1985).
[5]J. R. Tredicce, F. T. Arecchi, G. L. Lippi, and G. P. Puccioni, J. Opt. Soc. Am. B **2**, 173 (1985).
[6]J. R. Tredicce, F. T. Arecchi, G. P. Puccioni, A. Poggi, and W. Gadomski, Phys. Rev. A **34**, 2073 (1986).
[7]T. Midavaine, D. Dangoisse, and P. Glorieux, Phys. Rev. Lett. **55**, 1989 (1986).
[8]D. Dangoise, P. Glorieux, and D. Hennequin, Phys. Rev. Lett. **57**, 2657 (1987).
[9]H. G. Solari, E. Eschenazi, R. Gilmore, and J. R. Tredicce, Opt. Commun. **64**, 49 (1987).
[10]E. Eschenazi, H. G. Solari, R. Gilmore, and J. R. Tredicce (unpublished).
[11]H. G. Solari and R. Gilmore, Phys. Rev. A **37**, 3096 (1988).
[12]M. Henon, Commun. Math. Phys. **50**, 69 (1976).
[13]J. Guckenheimer and P. Holmes, *Nonlinear Oscillations, Dynamical Systems and Bifurcations of Vector Fields* (Springer-Verlag, New York, 1983).
[14]S. E. Newhouse, Topology **13**, 9 (1974); in *Dynamical Systems,* Vol. 8 of *Progress in Mathematics* (Birkhauser, Boston, 1980).
[15]B. D. Greenspan and P. J. Holmes, in *Nonlinear Dynamics and Turbulence,* edited by G. I. Barenblatt, G. Iooss, and D. D. Joseph (Pitman, Boston, 1983), p. 172.
[16]K. T. Alligood, L. Todeschini-Lalli, and J. A. Yorke (unpublished).
[17]C. Grebogi, E. Ott, and J. A. Yorke, Physica D **24**, 243 (1987).
[18]S. Smale, Bull. Am. Math. Soc. **73**, 747 (1967).
[19]J. R. Tredicce (private communication).
[20]T. P. Valkering, Physica D **27**, 213 (1987).
[21]R. Gilmore, *Catastrophe Theory for Scientists and Engineers* (Wiley, New York, 1981).
[22]J. Carr, *Applications of Center Manifold Theory* (Springer-Verlag, New York, 1981).
[23]C. Grebogi, E. Ott, and J. A. Yorke, Physica D **7**, 181 (1983).
[24]S. W. McDonald, C. Grebogi, E. Ott, and J. A. Yorke, Physica D **17**, 125 (1985).
[25]F. C. Moon and G.-X. Li, Phys. Rev. Lett. **55**, 1439 (1985).
[26]C. Grebogi, E. Ott, and J. A. Yorke, Phys. Rev. Lett. **56**, 1011 (1986).
[27]K. T. Alligood and J. A. Yorke (unpublished).
[28]I. B. Schwartz, Phys. Rev. Lett. **60**, 1359 (1988).
[29]K. T. Alligood, Trans. Am. Math. Soc. **292**, 713 (1985).

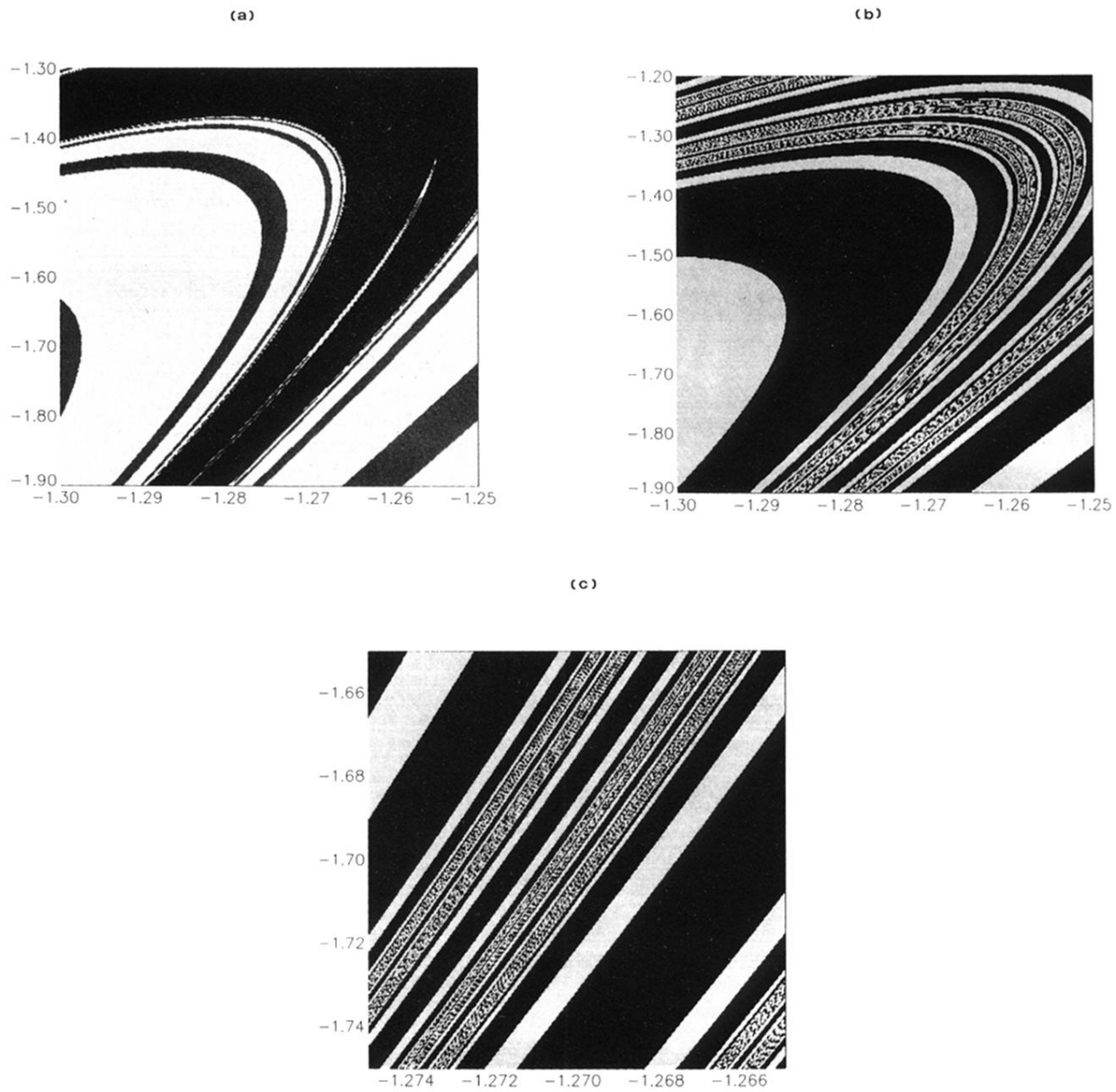

FIG. 20. Coexisting basins of attraction of the Henon map for $J=0.35$. (a) For $a=1.135$ there are three coexisting basins of period-1 (light), -3 (medium), and -4 (dark). (b) For $a=1.15$ the period-4 basin has disappeared, leaving in its place highly intertwined period-1 and -3 basins. (c) Enlargement of (b), showing intertwining of period-1 and -3 basins at an ever finer level.